

# ESRF Thermal Absorbers: Temperature, Stress and Material Criteria

L. Zhang, J. C. Biasci, B. Plan

European Synchrotron Radiation Facility, 6 rue Jules Horowitz, BP220, 38043 Grenoble Cedex, FRANCE  
Phone : +33 4 7688 2149, Fax : +33 4 7688 2585  
e-mail : zhang@esrf.fr

## Abstract

Many thermal absorbers are used to protect the ESRF storage ring vacuum vessels. These thermal absorbers are made of copper and water-cooled, should be designed to withstand the temperature and thermal stress induced by the high heat load. The mostly used design criterion is that the thermal stress in the absorber is lower than the elastic limit of the material. The X-ray heat load induced stress in the copper absorbers is compressive and concentrated in a small region near the surface. Various experiences at the ESRF and tests made on the thermal absorbers show that this criterion is too conservative for the synchrotron radiation thermal absorber. An audacious design criterion can be proposed: the maximum stress in the copper thermal absorber should be smaller than twice the ultimate tensile strength of the copper ( $\sigma_{\max}^{\text{VM}} < 400$  MPa for OFHC copper,  $\sigma_{\max}^{\text{VM}} < 850$  MPa for Glidcop).

**Keywords:** storage ring, absorber, heat load, stress, criteria

## 1. Introduction

In a storage ring based synchrotron light source, many thermal absorbers are used to protect the storage ring vacuum chambers. In general, these thermal absorbers absorb about 90% of the synchrotron radiation power generated by bending magnets. The rest of the power is absorbed by Front-End and beamline components. The thermal absorbers protecting the storage ring vacuum chamber can often be classified as 1) the crotch absorber - located downstream of the dipole vacuum chambers; 2) the distributed absorber – along the vacuum chambers; 3) the special absorbers – in the injection and RF cavity areas. These thermal absorbers are mostly made of copper, water-cooled and have to eliminate very high power density heat loads. For instance, a crotch absorber at the ESRF removes up to 8.16 kW of power at 200 mA current, with a peak linear power density of 72 W/mm or 177 W/mm<sup>2</sup> on the absorber. The thermal absorbers should be designed to withstand the temperature and thermal stress induced by the high heat load. Copper and Glidcop (dispersion strengthened copper) are widely used. Glidcop is renowned for its higher yield and ultimate tensile strength in comparison to OFHC (Oxygen-free High Conductivity) copper. Considerable efforts have been made in the design of the thermal absorbers, especially for crotch absorbers [1-5]. The aim of the design study was to reduce the maximum temperature and stress on the absorber. The commonly used design criterion is based on the principle that the maximum Von Mises stress in the absorber should be smaller than the yield strength of the material. Various experiences at the ESRF and tests made on the thermal absorbers show that this criterion is too conservative for the synchrotron radiation thermal absorber. Other criterion as a

rule of thumb used at APS is that the maximum temperature rise in the absorber should be below 300°C for Glidcop and 150°C for OFHC copper [2-3].

The thermal absorbers in the ESRF storage ring were designed for an e-beam current of 200 mA, twice of the beam current specification. In the scope of machine development, the e-beam current is planned to upgrade to 300 mA. The actual Glidcop crotch absorber is operated close to the elastic limit (yield strength) of the material at 200 mA. The thermal stress in a few absorbers made of OFHC copper at 200 mA is even greater than the yield strength. A question of safe operation at higher currents has to be addressed.

In this paper, we will first present the design of the majority of the storage ring thermal absorbers, FEA (Finite Element Analysis) results, and various tests or experience at the ESRF. Then, we will discuss the material limits appropriate for the thermal absorbers design for synchrotron light source.

## 2. ESRF Storage Ring Absorbers

The ESRF storage ring can be divided into 32 cells with 2 bending magnets per cell. Except the special regions (the injection and 3 acceleration RF cavities), all the cells are similar. The storage ring vacuum chambers were made of stainless steel. The thermal absorbers used to protect these vacuum chamber can be classified as three major types and some special absorbers for the special regions: 1) distributed absorber, 2) crotch absorber, 3) flat absorber, 4) special absorbers. All these absorbers are partially or totally made of copper or/and Glidcop, water-cooled, and designed such that there is no water-to-vacuum joint.

### 2.1 *Distributed Absorber*

The distributed absorber, illustrated in Fig.1-a, is the most common absorber. It is used to protect the quadrupole-sextupole vacuum chamber. A 6-mm thick copper plate was brazed on the inner side of the stainless steel vacuum chamber, and a water cooling copper tube was brazed on the outside of vacuum chamber.

### 2.2 *Crotch Absorber*

The crotch absorber, illustrated by Fig.1-b, is made of Glidcop and OFHC copper. It is located closest to the bending magnet. This absorber is the most critical one due to the high power density on it and the limited space for the installation. The front piece in 4mm thick Glidcop was brazed with square copper tubes, 10 tubes per segment. The three segments of the sub-assembly were brazed with another 10 mm thick copper plate on the back. Each segment is cooled independently.

The crotch absorber design was also adopted for the beam ports, Front-Ends, and some special crotch absorbers in the injection region.

### 2.3 Flat Absorber

The flat absorber, illustrated by Fig.1-c, is a 5 mm thick OFHC copper plate brazed on a stainless steel water box. It was installed in the crotch vessel, and in the section with bellows.

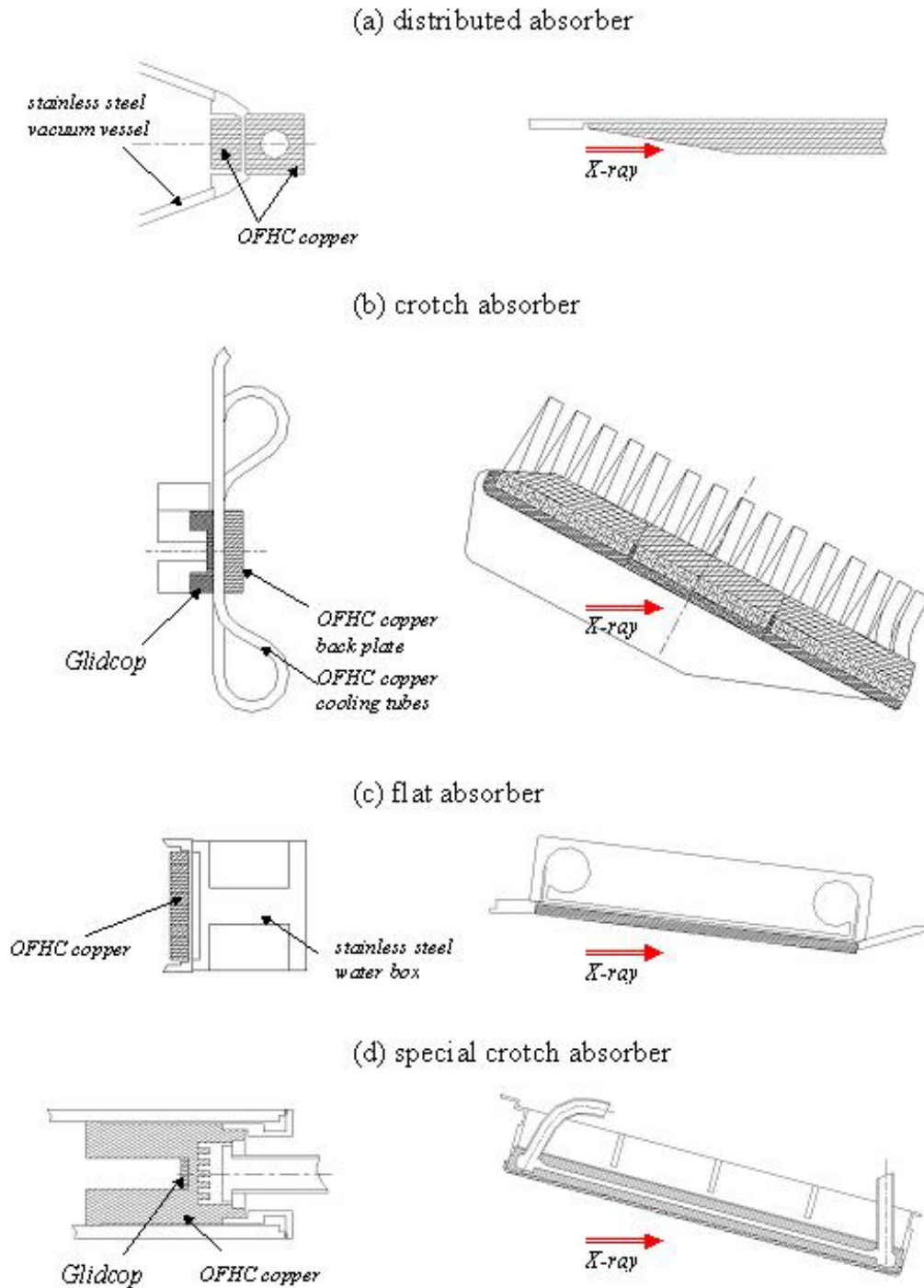


Fig. 1: Layout of principal ESRF absorbers in the storage ring.

## 2.4 Special Crotch Absorber

In the injection region, the crotch absorbers downstream of the two special dipole vacuum chambers are of a special design as illustrated in Fig.1-d. A fin pin structure was used in the cooling design. The X-ray beam incident angle as well as the power density on these special crotch absorbers is about 34% lower than on the common crotch absorbers (b). A special crotch absorber for the Graal experiment [6], called ‘Graal absorber’, is a similar design as illustrated by Fig.1-d. However, the X-ray beam incident angle as well as the power density on the Graal absorber is about twice that on the common crotch absorbers. The Graal absorber will be presented in the following sections.

In the injection region, there are some other absorbers similar to common crotch absorbers.

## 3. FEA (Finite Element Analysis)

### 3.1 Material Properties, Cooling and Heat Load

Thermal absorbers are made of Glidcop or/and OFHC copper. Stainless steel vacuum chambers can be partially included in the finite element modeling of the absorbers. Thermal mechanical properties (conductivity, thermal expansion coefficient, and modulus of elasticity) of these materials (Table 1) vary less than 10% with temperatures in the range of 20 to 400°C, and will be considered as constant in the FEA.

Table 1: Thermal Mechanical Properties of Copper, Glidcop and Stainless Steel

	<i>Copper</i>	<i>Glidcop</i>	<i>Stainless steel</i>
<i>Thermal conductivity (W/mm/°C)</i>	<i>0.38</i>	<i>0.34</i>	<i>0.017</i>
<i>Thermal expansion coefficient (μm/m/°C)</i>	<i>17</i>	<i>17</i>	<i>17</i>
<i>Modulus of elasticity (GPa=kN/mm<sup>2</sup>)</i>	<i>130</i>	<i>130</i>	<i>200</i>
<i>Poisson ratio</i>	<i>0.34</i>	<i>0.34</i>	<i>0.33</i>

All the thermal absorbers at the ESRF are cooled by water. In most cases, a cooling coefficient of  $h=0.02$  W/mm<sup>2</sup>/°C was applied to the cooled wall. In practice, the water flow rate was designed to easily achieve the necessary cooling efficiency. Note that the thermal stress from FEA is almost independent of the cooling coefficient  $h$ . The maximum temperature of the thermal absorbers  $T_{\max}$  and of the cooled wall  $T_{w_{\max}}$  vary with  $h$ .

The angular power density from the bending magnet radiation in the horizontal plane is constant and calculated by

$$P_{\theta}(\text{W/mrad}) = 4.224 B(\text{T}) E(\text{GeV})^3 I(\text{A}) \quad (1)$$

Heat load on the absorbers is a thin horizontal line, the width of this line is  $\sqrt{2\pi}\sigma$ . The power distribution across this line is Gaussian, with a standard deviation  $\sigma$ . At normal incidence, the linear power density  $P_l$  and power density  $P_a$  are respectively

$P_l = P_\theta/d$  and  $P_a = \frac{P_l}{\sqrt{2\pi}\sigma} = \frac{P_\theta}{d\sqrt{2\pi}\sigma}$  where  $d$  is the distance between the absorber and the source point of the bending magnet. The standard deviation  $\sigma$  depends on machine parameters and the distance  $d$ . For short distance  $d$ , the value of  $\sigma$  varies significantly on the absorber, for instance,  $\sigma=0.12 - 0.21$ mm for crotch absorber ( $d=1.4-2.5$ m). For long distances  $d$ , the value of  $\sigma$  is almost constant on the absorber, for instance,  $\sigma=0.52 - 0.55$ mm for distributed absorber upstream of the ID vacuum chamber ( $d\sim 6$ m). For  $\sigma$  in a range such as 0.12-0.55 mm, the thermal stress does not significantly vary with  $\sigma$ . Therefore, the linear power density is a good measure for the heat load on the thermal absorbers. In general, FEA of the thermal absorbers is performed with variable power density: Gaussian distribution in the vertical direction and linearly variable distribution in the horizontal direction.

### 3.2 Finite Element Modeling of the Absorbers

Since the construction of the ESRF, huge progress has been achieved in computer and FEA software prowess.

Much finer FEA can be performed today than 10 years ago. The crotch absorber was modeled and analyzed in two or three separate parts during the design phase. Today the FEA of the whole crotch absorber was carried out with much more accurate power distribution (Fig.2). The size of the model shown in Fig. 2 is about 100 times the size of the finite element model that we treated in 1989-1990.

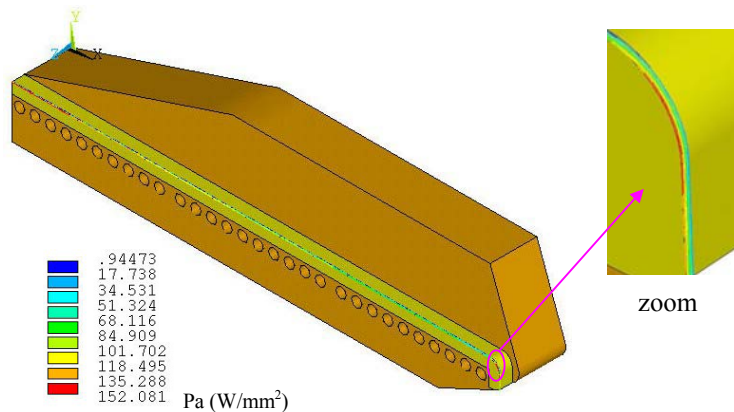


Fig. 2: Finite Element model of the crotch absorber (orange for OFHC copper, green-yellow for Glidcop). Power distribution is Gaussian in vertical direction (z-axis) and linearly variable in horizontal direction (x-axis)

As the e-beam lifetime is much longer than the thermal diffusion time in the absorbers, only steady state at maximum e-beam current (200 mA) will be considered. The thermal deformation is always assumed to be elastic. If the computed stress is larger than the elastic limit of the material, the computed stress is only an apparent stress related to the thermal strain, and is not a real stress. Therefore, the calculated stress of the absorbers could be larger than yield strength, even larger than the tensile strength of the material. No mechanical constraint was applied to the FE model. The calculated stress is thus pure thermal stress. In the case of symmetry, only half or quarter of the absorber is modeled, as shown in Fig. 2 for half a crotch absorber. Variable meshing has always been preferred in order to have a much thinner mesh in the region with heat load (high temperature gradient and high stress) than in the other regions.

### 3.3 FEA Results

FEA has updated one of each type of absorbers in the storage ring, with maximum power density on each type. Results in maximum temperature of the absorber  $T_{max}$  and of the cooled wall  $T_{w_{max}}$ , and in maximum Von Mises stress  $\sigma_{max}^{VM}$  are summarized in Table 2, as well as peak power densities  $P_l$ ,  $P_a$  and standard deviation  $\sigma$  on the absorbers. Data in Table 2 was organized in 2 blocks: one for Glidcop absorbers and the other for OFHC copper absorbers. The maximum temperature and stress on the crotch absorbers are respectively  $T_{max}=400^\circ\text{C}$  and  $\sigma_{max}^{VM}=408$  MPa. Results on the Graal absorber reached astonishing levels:  $T_{max}=587^\circ\text{C}$  and  $\sigma_{max}^{VM}=828$  MPa. This Graal absorber is a special crotch absorber for Graal

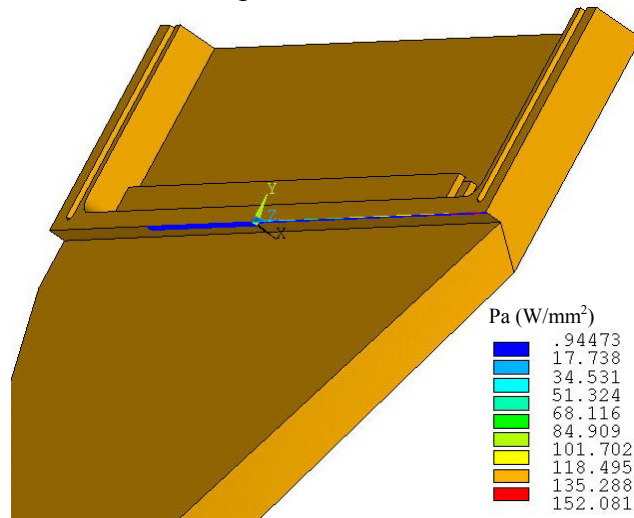


Fig. 3: Finite Element model of the Graal absorber. Power distribution is Gaussian in vertical direction (x-axis) and variable in horizontal direction (z-axis)

experiment [6]. A FEA model is shown in Fig. 3. The bending magnet radiation power was mainly concentrated on half of the absorber with a peak power density of  $321 \text{ W/mm}^2$ , twice that of the common crotch absorber. This was mainly due to the fact that the X-ray beam incident angle ( $45^\circ$ ) on the Graal absorber is about twice that on the

common crotch absorber (22.8°).

Table 2: FEA Results for One of Each Type of Absorber in the Storage Ring

material : **Glidcop (+OFHC)**

type (material)	identification	$\sigma$	$P_l$	$P_a$	$P_{total}$	$T_{max}$	$T_{w_{max}}$	$\sigma_{max}^{VM}$	comments
		mm	W/mm	W/mm <sup>2</sup>	W	°C	°C	MPa	
crotch	CV 13	0.19	72	153	7 189	<b>400</b>	<b>121</b>	<b>408</b>	OK
graal	C7/CV06 (old)	0.11	90	321	10 121	<b>587</b>	<b>211</b>	<b>828</b>	safe ~ 5 yrs

material : **OFHC**

tested crotch <b>with IDs</b>	1 U34/12			45	2 608	<b>264</b>	<b>59</b>	<b>428</b>	safe ~1 month
	2 U34/12+12.5mm			88	4 630	<b>464</b>	<b>88</b>	<b>786</b>	safe 2~3 hours
special crotch	C3/d_strm-K2	0.14	52	151	3 434	<b>261</b>	<b>83</b>	<b>414</b>	OK, <i>upgraded</i>
distributed	CV15A	0.23	11	19	1 182	<b>89</b>	<b>32</b>	<b>80</b>	OK
	C3/d_strm-K2	0.15	18	49	243	<b>117</b>	<b>34</b>	<b>108</b>	OK
flat	CV14	0.13	15	45	2 276	<b>148</b>	<b>38</b>	<b>221</b>	OK

common crotch absorber (22.8°).

The maximum stress on the OFHC copper absorber is also very high. The extreme case is the special absorber installed in the injection region downstream of the kicker No2

(C3/d\_strm-K2). The thermal stress reaches  $\sigma_{max}^{YM}=414$  MPa. More details on this absorber will be reported in section 4.4. Table 2 also shows FEA results for the OFHC copper crotch absorber tested with undulator power. These tests will be described in section 4.3.

#### 4. Tests and Experiences with Absorbers

##### 4.1 Flat Absorber Tests with e-beam

In 1991, the ESRF was in the construction phase. To assess the reliability of the thermal absorbers, a water-cooled flat absorber (Fig. 4-a) was tested with an e-beam gun normally used for e-beam welding. The e-beam was used as a heat load source. Its spot size is about  $D=0.8$  mm in diameter at the position of the absorber. To simulate the power distribution of the X-ray on the absorber, the e-beam was swept along the absorber surface over a length of  $L=50$  mm with a frequency of 400 Hz. The  $130 \times 30$  mm<sup>2</sup> of absorber surface was divided into 2x5 test areas (see Fig.4-b), on which different e-beam powers were applied. The total absorbed power  $P$  by the flat absorber is about 66% of the applied e-beam power. The power density of the e-beam spot is  $P_{a-spot} = \frac{4P}{\pi D^2}$ . Tests

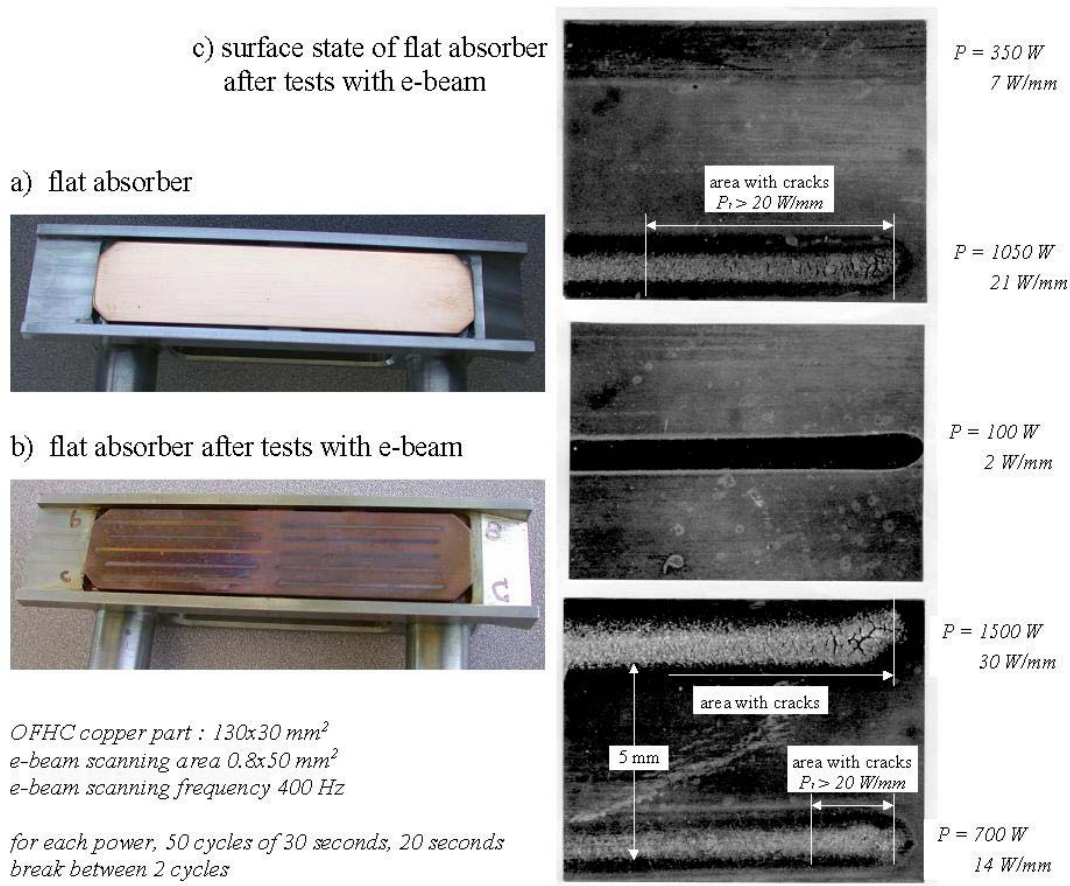


Fig. 4: Flat absorber before a) and after b) test with an e-beam gun, and c) surface states after tests. Cracks are clearly visible in the area of  $P_i > 20$  W/mm.

were made with 50 thermal cycles on every test area with corresponding power. Each thermal cycle consists of 30 seconds of e-beam sweeping, and 20 seconds of break. With assumption of a sinusoid sweeping speed  $V(t) = V_0 \sin \omega t$ , it can be shown that the time-averaged linear (absorbed) power density  $P_l$  on the test area is

$$P_l = \frac{2P}{\pi L \sqrt{1 - (2x/L)^2}} \quad (2)$$

The surface states after tests with e-beam are shown in Fig. 4-c. Absorbed power and average linear power density are indicated beside the traces hit by the e-beam. Cracks were observed on the absorber surface in the areas of  $P=700, 1050, 1500$  W, especially at the end. The higher the power is, the longer the crack area is. Combining the length of the crack area and the power distribution given in Eq. (2), we deduced that the crack appears in the area with a linear power density  $P_l > 20$  W/mm, or a power density of  $25$  W/mm<sup>2</sup>. The power density of the e-beam spot is  $P_{a-spot} = 1400$  W/mm<sup>2</sup> for  $P=700$  W. The time-averaged (linear) power density is much lower than this power density of the e-beam spot. The calculated thermal stress with a uniform power density of  $P_l = 20$  W/mm is  $\sigma_{max}^{JM} = 295$  MPa. Note that the value of the (linear) power density corresponds to effectively absorbed power density, and is time-averaged. However, values given in Table 2 correspond to X-ray incident power and power densities. In general, the incident power is not totally absorbed by the thermal absorbers. It was conservative or safe to take the value of  $P_l = 20$  W/mm as the upper power limit in the flat absorber design. Also the value of  $\sigma_{ultimate}^{JM} = 295$  MPa was considered as the thermal stress limit for the OFHC copper absorbers.

#### 4.2 Graal Absorber at the ESRF

As mentioned in section 3.3, the Graal absorber, a special crotch absorber for the Graal experiment [6], was a design shown in Fig. 3 and Fig. 1-d. This absorber was installed in summer 1994 and replaced in December 1999 by a common crotch absorber in the frame of Graal experiment re-design. Temperature and stress of the old Graal absorber reached a very high level from FEA:  $T_{max} = 587^\circ\text{C}$  and  $\sigma_{max}^{JM} = 828$  MPa. This calculated thermal stress is significantly higher than the yield and tensile strengths of the Glidcop. After replacement, the Graal absorber was analyzed in-

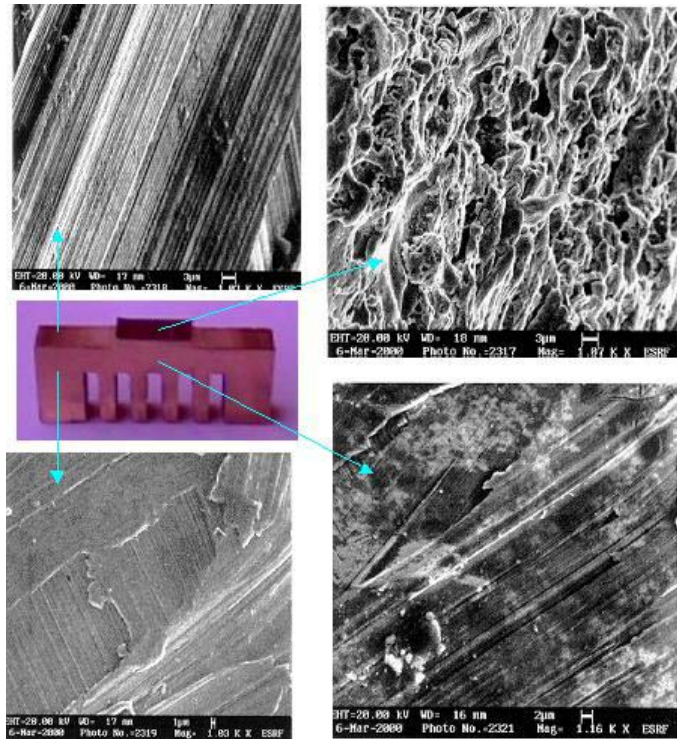


Fig. 5: Surface states of the Graal absorber: scanning electron microscope photos.

house using a scanning electron microscope. Photos of the surface state at different faces of the cut piece (Fig. 5) do not show any cracks. Only porous oxidization was observed on the top surface in the X-ray beam impingement area. More detailed analyses were also performed by material structure and behavior laboratory [7]. This study confirmed that the included aluminum in the Glidcop is mostly small in size (20 nm), with a few in size of 1 to 2  $\mu\text{m}$ . A porous oxidized thin layer with enriched aluminum was observed on the cooling fin pin side. The final conclusion was that no cracks and nor degradation were observed on the cut copper piece from the Graal absorber. It should be pointed out that this absorber had been operating safely for 5 years.

### 4.3 Crotch Absorber Tests with Undulator Beam Power

In the ESRF machine development projects, upgrading the e-beam current from 200 to 300 mA was one of targets. This e-beam current upgrade means that the synchrotron radiation power will be increased by 50%. Since the actual crotch absorber made of Glidcop is operated with a maximum stress close to the elastic limit of the material at 200 mA, a safe operation at a higher current has to be questioned. In order to assess the temperature and stress limits for the copper absorbers, tests with an OFHC copper crotch absorber were carried out in 2001 on a test beamline with possible three segments of U34 undulators. The crotch absorber was placed at 16 m from the center of undulators. The insertion device at its minimum gap (11mm) can generate 10 kW of total power and 1100 W/mm<sup>2</sup> power density at normal incidence at the position of the absorber. The power distribution of the undulator radiation is approximately Gaussian in both the vertical and transverse directions. The standard deviation is respectively 0.72 and 1.68 mm in vertical and transverse directions. The crotch absorber was oriented to have an X-ray incident angle (horizontally) of 7.5 degrees. Indeed, the power distribution of the undulator radiation on the test crotch absorber is different from the bending magnet radiation on the common crotch absorber, shorter in the horizontal direction and larger in the vertical direction. The peak power densities are comparable in both cases. However, the temperature and stress induced by the undulator radiation on the test crotch absorber can be significantly higher than those induced by the bending magnet at 300 mA on the common crotch absorber. Power from undulators calculated by SRW software [8] was compared to the heat power evacuated by cooling water at different undulator gaps. Calculated power by SRW is about 10% higher than evacuated power by cooling water. The trends of the power versus undulator gap are well correlated between the SRW and measurement results. The test of the crotch absorber with undulator beamline was also used to check

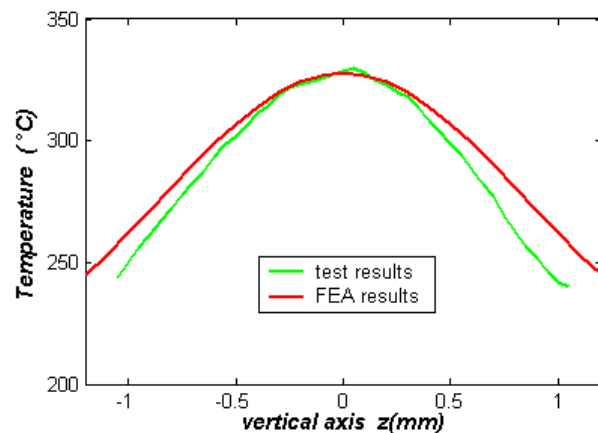


Fig. 6: Surface temperature profile of the crotch absorber tested with undulator radiation from measurement by infrared pyrometer and from finite element simulation

finite element modeling. The temperature on the absorber surface was measured using an infrared pyrometer, and was consistent with finite element simulations (Fig. 6). This partially validates the finite element modeling. As the thermal stress is locally concentrated in the area exposed to the X-ray power, strain gauges are not appropriate for the thermal stress measurement of the thermal absorbers. The data of thermal stress of the absorber are thus FEA results.

The OFHC copper crotch absorber was exposed to the power emitted by one segment of U34 undulator during about 1 month, and two segments during 2 to 3 hours. No any particular behavior was observed during these tests, such as sudden temperature and/or pressure increases. The crotch absorber safely withstood the high heat load without any notable damage. The maximum temperature and stress on the absorber from FEA are given in Table 2 for test conditions.

#### 4.4 Special Crotch C3/d\_strm-K2

A special crotch absorber (Fig. 7) of the same design as the common crotch absorber but shorter was made of OFHC copper and installed in the injection region downstream of the kicker No2 (C3/d\_strm-K2). The first crotch absorbers were all made of OFHC copper and replaced by Glidcop design after several months of machine commissioning in 1992. This special crotch absorber C3/d\_strm-K2 was only replaced in August 2002. A thin trace on the center surface of the absorber was marked by the synchrotron radiation. Observation under the optical microscope with a magnification of 40 did not show cracks on the X-ray illuminated area. Destructive test would be necessary for deeper analysis. This absorber will be kept as a spare part.



Fig. 7: Special crotch absorber C3/d\_strm-K2

## 5. Design Criteria for Thermal Absorbers

The commonly used thermal absorber design criteria [1,4-5,9] are that

- The maximum temperature of the absorber  $T_{max}$  should be significantly lower than melting point of the copper, or brazing temperature
- The maximum cooling wall temperature  $T_{w_{max}}$  should be lower than water boiling temperature  $T_{boiling}$  at the pressure of the water in the cooling tubes
- the maximum Von Mises stress in the absorber  $\sigma_{max}^{VM}$  should be lower than the yield strength of the material, or ultimate tensile, fatigue strengths

Other criteria, such as maximum temperature rise in the absorber less than 300°C for Glidcop and 150°C for OFHC copper are also used at APS [2-3].

There are many data of yield strength and ultimate tensile strength of Glidcop and OFHC copper in literature [1-2, 9-13]. These data depend on the composition, shape, thermal treatment, and temperature. As an indication, the yield and ultimate tensile strengths at room temperature are respectively 45 and 210 MPa for annealed OFHC

copper [11], 331 and 413 MPa for Glidcop [12]. These values could be higher for different temper and cold work of the copper.

The ESRF absorbers were, in general, designed respecting the commonly used criteria. However, the stress criteria were not as restrictive as stated above. The effectively used stress criteria were:

- Maximum Von Mises stress in the Glidcop crotch absorbers should be smaller than 430 MPa for temperature under 400°C, and 400 MPa for temperature under 500°C. These stress values correspond to the yield strength after the first thermal cycle [1] :  $S_{yield}(cold)+S_{yield}(hot)$ .
- For the OFHC copper absorbers, the stress criterion was based on the results of tests made with e-beam in 1991 :  $\sigma_{max}^{VM} < 295$  MPa. More practically,  $P_l < 20$  W/mm was applied in the design of the flat and distributed absorbers.

Since the operation of the ESRF machine in 1992, all of the thermal absorbers in the storage ring have been working with no failure.

For the flat absorbers, the maximum incident linear power density is  $P_l=15$  W/mm and maximum stress is  $\sigma_{max}^{VM}=221$  MPa, on the CV14 flat absorber (Table 2). For the distributed absorber, the linear power density is not very high except in the leading slope as shown in Fig.1-a. The maximum stress on the distributed absorber is  $\sigma_{max}^{VM}=108$  MPa. The special crotch absorber C3/d\_strm-K2 was in OFHC copper and replaced by a Glidcop one only in August 2002. The calculated thermal stress in this OFHC copper absorber reached  $\sigma_{max}^{VM}=414$  MPa, which is much higher than the yield and ultimate strengths of the OFHC copper. This special crotch absorber has worked with no failure over the ten years of machine operation. The recent replacement was made in the scope of a machine e-beam current upgrade from 200 to 300 mA. The temperature and stress on the OFHC copper crotch absorber tested with undulator beamline reached  $T_{max}=264^\circ\text{C}$  and  $\sigma_{max}^{VM}=428$  MPa for 1 segment of U34 at gap 12mm during one month of machine operation,  $T_{max}=464^\circ\text{C}$  and  $\sigma_{max}^{VM}=786$  MPa for two segments of U34 at gap 12 and 12.5 mm for two to three hours. The crotch absorber safely withstood the high heat load without any notable damage. It is clear that a few of OFHC copper absorbers withstand much higher thermal stresses than yield and ultimate strengths of the OFHC copper. The tests made in 1991 with scanning e-beam on the flat absorber led to material damage on the absorber surface. Cracks were observed in the area with stress larger than 295 MPa. The value of this stress is lower than the stress on the C3/d\_strm-K2 OFHC copper absorber and on the OFHC crotch absorber tested with undulator X-ray power. This is probably due to the consideration of time-averaged scanning e-beam power density. However, the instantaneous power density of the spot e-beam is much higher (about  $50/0.8=62.5$  times) than time-averaged power density.

For the common crotch absorber in Glidcop, the maximum temperatures on the absorber and on the cooled wall are respectively  $T_{max}=400^\circ\text{C}$  and  $T_{wmax}=121^\circ\text{C}$ , the maximum thermal stress is  $\sigma_{max}^{VM}=408$  MPa. These data are within the design criteria. The old Graal absorber was, indeed, in Glidcop. However the temperature and stress from FEA reached very high levels:  $T_{max}=587^\circ\text{C}$ ,  $T_{wmax}=211^\circ\text{C}$ , and  $\sigma_{max}^{VM}=828$  MPa. This calculated thermal stress is significantly higher than the yield and tensile strength of

the Glidcop. However, this absorber had operated safely for more than 5 years, and micro-structural analyses do not show any cracks, any material degradation in the absorber. The maximum cooled wall temperature  $T_{w_{max}}=211^{\circ}\text{C}$  is higher than  $T_{boiling}=183^{\circ}\text{C}$  of the water boiling temperature at 10 bars (the pressure of the cooling water). The cooled wall temperature above water boiling temperature is localized in a small region. The beginning of the boiling in a small region was not destructive due to the cooling coefficient enhancement.

The thermal stress in the absorbers induced by synchrotron radiation is mainly compressive, concentrated in a narrow and long region near the surface hit by the X-ray. Compressive stress is less critical than the tensile stress. Copper is a ductile material. The concentrated stress can be significantly larger than the yield strength without any notable stress increase. The X-ray heat load induces basically localized thermal strain in the thermal absorbers. If the strain is larger than the elastic limit, plastic deformation can be operated in the small region hit by X-ray. Results of tests and experiences with some ESRF thermal absorbers lead to the following conclusion: copper thermal absorbers can probably withstand a concentrated and compressive thermal stress twice that of the ultimate tensile strength, about 400 MPa for OFHC copper and 850 MPa for Glidcop for a number of cycles larger than  $10^4$ . This number of cycles corresponds to ten years of machine operation at the ESRF. The total number of e-beam injections is about 1000 times per year. These data are not the ultimate limits for copper thermal absorber. A dedicated in-house test beamline with three segments of undulator will be used to test copper thermal absorbers. Samples representing typical thermal absorbers will be subjected to the very high ID power cycling. These tests are expected to establish the ultimate stress limits of the copper thermal absorbers.

## 6. Concluding Remarks

The design of the thermal absorbers for the ESRF storage ring has been reviewed. The finite element analyses of these absorbers have been updated. The thermal stress in some absorbers exceeds the yield and ultimate tensile strengths of the coppers. Apparent stresses up to twice those of the ultimate tensile strength of the coppers have been recorded in the special crotch absorbers (Graal Glidcop absorber, C3/d\_strm-K2 OFHC copper absorber). These thermal absorbers had been in service for five or ten years without failure. The X-ray heat load induced stress in the copper absorbers is compressive and concentrated in a small region near the surface. The conventional design criterion – maximum Von Mises stress lower than yield strength of the material - is too conservative. An audacious design criterion can be proposed:

**The maximum stress in the copper thermal absorber should be smaller than twice that of the ultimate tensile strength of the copper ( $\sigma_{max}^{VM} < 400$  MPa for OFHC copper,  $\sigma_{max}^{VM} < 850$  MPa for Glidcop).**

## **7. Acknowledgement**

Authors gratefully acknowledge I. Snigireva for microscope photos in Fig. 5 and Fig. 7.

## **8. References**

- [1] G. Marot, "Design of the ESRF absorbers," ESRF internal report, 1989.
- [2] I. C. Sheng, S. Sharma, R. Rotela and J. Howell, "Thermomechanical analysis of a compact-design high heat load crotch absorber," Proc. of the 1995 Particle Accelerator Conference, Dallas, Texas (1996) 816-818.
- [3] S. Sharma, R. Rotela and A. Barcikowski, "High heat-load absorbers for the APS storage ring," Proc. of MEDSI2000, Switzerland (2000).
- [4] S. Hermle, D. Einfeld and E. Huttel, "Layout of the absorbers for the synchrotron light source ANKA," Proc. of the 1999 Particle Accelerator Conference, New York (1999) 1360-1362.
- [5] L. Zhang, "Preliminary absorber design for the ultimate storage ring light source," Proc. of the 2002 European Particle Accelerator Conference, Paris (2002).
- [6] <http://www.esrf.fr/info/science/newsletter/apr98/DOSEXP/GRAAL.HTM>
- [7] I. Touet, "Expertise sur pièce de cuivre," SPCM/LSCM/IT/2000-067, CEA-CEREM-Laboratoire structure et comportement des matériaux, (2000).
- [8] [http://www.esrf.fr/machine/groups/insertion\\_devices/Codes/SRW/srwindex.html](http://www.esrf.fr/machine/groups/insertion_devices/Codes/SRW/srwindex.html)
- [9] M. Choi, "Crotch thermal studies," Accelerator advisory committee meeting, APS, Chicago (1990).
- [10] J. J. Stephens and D. T. Schmale, "The effect of high temperature braze thermal cycles on mechanical properties of a dispersion strengthened copper alloy," Sandia report SAND87-1296, Albuquerque, New Mexico, (1999).
- [11] "Copper data," CDA (Copper Development Association, <http://www.copper.org/>) TN20, (1975).
- [12] "Glidcop," SCM Metal Products, Inc, Cleveland, Ohio, (2000).
- [13] <http://www.matls.com/search/SearchSubcat.asp>